Numerical simulation of external flow around cylinder using improved lattice Boltzmann method

Mohsen Soufi Boubakran, Iraj Mirzaee

Department of Mechanical Engineering, Urmia University, Urmia, Iran
E-mail: mohsen.soufi2015@gmail.com

Published in *The Journal of Engineering*; Received on 18th December 2017; Accepted on 12th February 2018

Abstract: In this study, incompressible and viscous external flow around a cylinder is simulated using the lattice Boltzmann method. The surface of cylinder is considered to be a rigid immersed body in the fluid flow. The fluid flow field is discretised by a uniform and fixed Cartesian mesh but there are difficulties in the modelling of curved boundaries. As a result, the cylinder surface is extrapolated by macroscopic properties at boundary nodes. On the other hand, to well treat with boundary condition of the cylinder surface and in the meantime, to save the computational effort, an innovation is applied in this research which solves this problem by introducing a new curved boundary condition to improve computational accuracy in lattice Boltzmann simulations. However, this method can be extended to other physical fields as well as fluid flow. The present results have been compared with the available numerical results which show good agreements.

1 Introduction

The lattice Boltzmann method (LBM) is a useful simulation technique for numerically solving flow problems [1–4]. This method is also feasible as a simulation technique for systems such as a suspension of solid particles or a polymeric liquid. LBM was first developed by Mcnamara and Zanetti [5] in 1998 to solve the problems with lattice gas automata method. Unlike conventional numerical schemes based on the discretisation of macroscopic continuum equations, the LBM is based on microscopic models and mesoscopic kinetic equations. LBM recovers the Navier–Stokes using Chapman–Enskog expansion. One of the most important benefits of lattice Boltzmann is the explicit form of governing equation and easy solution of parallel equations and boundary conditions employment on the curved boundaries. The lattice Boltzmann applications are in the fields of incompressible flows simulation in the complicated geometries like blood flow in vessels, multiphase flows, free convection problems, moving boundaries, chemical reactions, porous media flows, suspended particles, Magneto Hydro Dynamics (MHD) flows, non-Newtonian fluid flows, large eddy simulations, turbulence flows in aerodynamics and other applications [6–8]. It was also developed into an efficient method for solving the problems including the interaction of flow and solid [9–11]. Cheng and Zhang [10] have proposed a proper model to simulate the fast boundary movements and a high pressure gradient occurred in the fluid–solid interaction. In their research, mitral valve jet flow considering the interaction of leaflets and fluid has been simulated. Recently, the lattice Boltzmann has been combined with immersed boundary method to use for simulating the movement and changing the shape of immersed boundaries. This method is a combination of a mathematical formulation and a numerical method. Mathematical formulation of immersed boundary method included Eulerian variables. Discrete equations in place of a lattice of immersed boundary method use a Cartesian grid for Eulerian variables and a Lagrangian one for immersed boundaries. Lagrangian boundaries can move freely within the Cartesian grid and there is no need to adapt the Eulerian grids. Many studies have been conducted in this area.

Dupuis *et al.* [12] studied the flow over an impulsively started cylinder at moderate Reynolds (Re) number. They investigated how the coupling method of the forcing term between the Eulerian and Lagrangian grids could affect the results. Zhang *et al.* [9, 13] studied the dynamic behaviour of red blood cell in shear flow and channel flow and investigated several hemodynamic and rheological properties. Cheng and Zhang [10] have proposed a proper model to simulate the fast boundary movements and high pressure gradient occurred in the fluid–solid interaction. In their research, mitral valve jet flow considering the interaction of leaflets and fluid has been simulated.

However, studies on the unlimited (infinite range) are concentrated on the experiments. In the limited work that was done on simulating of flow around a cylinder, numerical methods rather than lattice Boltzmann were used. Therefore, in this paper shear flow around a cylinder was studied using improved lattice Boltzmann and the results were compared with experimental findings. In this research, a replaced mesoscopic method called LBM is used. In this method, the flow is considered as a cluster of particles which can collide with each other. The main advantage of this method is the relative simplicity in implementing and compatibility with the desired geometries. The main novelty of this paper is to implement a new designed boundary condition for the curved cylinder surface. Some researchers use other methods such as immersed boundary or immersed interface methods for simulating the flow around immersed objects like cylinder. However, these methods need more efforts to implement with respect to lattice Boltzmann. So in the present study, an improvement is applied to LBM to increase its benefits.

2 Governing equations

In recent decades, the LBM has been highly regarded. This method is a reliable alternative to conventional methods of Computational Fluid Dynamics (CFD) to solve complex problems of the flow which has been used in many engineering applications [14]. Unlike conventional methods that consider fluid as integrated, in this method the flow of virtual particles is considered. So LBM can model the relationship between particles which is the base for multi-phase flows. When Mach numbers (the ratio of average flow speed to the speed of sound) and Knudsen (the ratio of the mean free path to the length flow characteristic) are small enough, Boltzmann equations are a good approximation for Navier–Stokes equations.

The final form of Navier–Stokes equations will be as follows:

$$\nabla \cdot \boldsymbol{u} = 0 \tag{1}$$

$$\rho\left(\frac{\partial \boldsymbol{u}}{\partial t} + \boldsymbol{u} \cdot \nabla \boldsymbol{u}\right) = -\nabla p + \nu \nabla^2 \boldsymbol{u} \tag{2}$$

doi: 10.1049/joe.2017.0894

In the above equation, ρ and ν are the dynamic viscosity of the fluid mass and density, respectively. In addition, $\boldsymbol{u} = (u, v)$, p and t show the velocity, pressure and time, respectively.

As noted earlier in LBM, fluid is composed of virtual particles which can collide. In addition to the spatial position, the speed is also discrete in this method. This implies that the particles only move along directions marked with discrete speeds. The discrete Boltzmann equations by expanding the Chapman–Enskog results in Navier–Stokes equations (1) and (2) are written as follows:

$$f_i\left(\boldsymbol{x} + \hat{e}_i\Delta t, t + \Delta t\right) - f_i(\boldsymbol{x}, t) = -\frac{f_i(\boldsymbol{x}, t) - f_i^{\text{eq}}(\boldsymbol{x}, t)}{\tau} \tag{3}$$

where $f_i(\boldsymbol{x}, t)$ is the particle distribution function and $\hat{e}_i$ is speed of position $\boldsymbol{x}$ at time of t. Δt is the time step, $f_i^{\text{eq}}(\boldsymbol{x}, t)$ is the equilibrium distribution function and time τ indicating the non-dimensional relaxation time in the Boltzmann equation. In the present work, LBM is used with two-dimensional D2Q9 model; there are eight moving particles and a stationary one in this model and is shown in Fig. 1. The velocities of the particles can be written in the form of the following equation [14]:

$$\hat{e}_i = \begin{cases} (i, i), & i = 0 \\ \left(\cos\dfrac{\pi(i-1)}{2}, \sin\dfrac{\pi(i-1)}{2}\right)c, & i = 1-4 \\ \sqrt{2}\left(\cos\dfrac{\pi(i-9/2)}{2}, \sin\dfrac{\pi(i-9/2)}{2}\right)c, & i = 5-8 \end{cases} \tag{4}$$

In this equation, $c = \Delta x/\Delta t$ and Δx are the intervals between two consecutive nodes in the Eulerian grid. The equilibrium distribution function is written in the form of the following equation:

$$f_i^{\text{eq}} = w_i\rho\left[1 + 3\frac{(\hat{e}_i \cdot \boldsymbol{u})}{c^2} + \frac{9}{2}\frac{(\hat{e}_i \cdot \boldsymbol{u})^2}{c^4} - \frac{3}{2}\frac{|\boldsymbol{u}|^2}{c^2}\right] \tag{5}$$

where w_i is the weight coefficient with the following values:

$$\begin{cases} w_0 = 4/9 & \\ w_i = 1/9 & \text{if } i = 1-4 \\ w_i = 1/36 & \text{if } i = 5-8 \end{cases} \tag{6}$$

The elastic force in the lattice Boltzmann equation is defined as

$$F_i = \left(1 - \frac{1}{2\tau}\right)w_i\left[\frac{3(\hat{e}_i - \boldsymbol{u})}{c^2} + \frac{9(\hat{e}_i \cdot \boldsymbol{u})}{c^4}\hat{e}_i\right] \tag{7}$$

Kinematic viscosity in D2Q9 model is written as follows and it is related to the non-dimensional time of τ. If $\tau > 1$ is selected, the results will be unreliable. In general, it is better to select $0.5 < \tau \leq 1$. In the present work $\tau = 1$ has been selected

$$\nu = c_s^2\left(\tau - \frac{1}{2}\right) \tag{8}$$

Macroscopic fluid density is obtained by the following equation:

$$\rho = \sum_{i=0}^{8} f_i \tag{9}$$

In addition, the macroscopic velocity of $\boldsymbol{u}$ is

$$\boldsymbol{u} = \frac{1}{\rho}\left[\sum_{i=0}^{8} f_i\hat{e}_i\right] \tag{10}$$

It should be noted that although the LBM is simulating the incompressible isothermal flows, density is not constant. In addition, the pressure does not appear clearly in any of the above equation. In this method, the following equation is used to calculate the pressure:

$$p = \rho c_s^2 \tag{11}$$

where p is the unit pressure in the lattice, $c_s = c/\sqrt{3}$ is the sound velocity in lattice and ρ is the lattice density. In the lattice Boltzman $\Delta x = \Delta t = 1$, therefore $c_s = 1/\sqrt{3}$. In addition, the relation between physical pressure p_p and lattice pressure p is obtained by

$$p_p = \rho_p c_{s,p}^2 = \rho_p\left[c_s^2\left(\frac{\Delta x_p}{\Delta t_p}\right)\right]^2 = \rho_p\left(\frac{\Delta x_p}{\Delta t_p}\right)^2\frac{p}{\rho} \tag{12}$$

where the index p represents the physical quality.

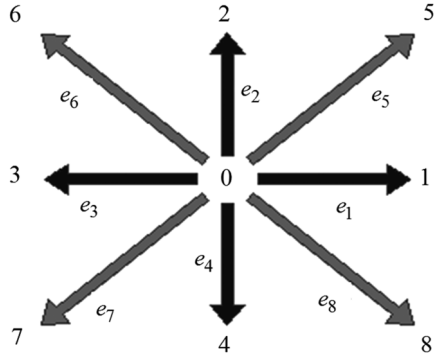

Fig. 1 *Velocities in D2Q9 model*

3 Implementation of the boundary curve in LBM

Two-step algorithm of colliding-streaming which has been introduced in (3) in LBM requires a Cartesian grid with similar grid node distance. The simulation of fluid flow is limited to simple geometries of sharp edges.

Faced with more complex geometries including curved boundaries using such a girding due to lack of full compliance between the curved boundaries and grid nodes has no results except that approximate of boundaries of the curve with broken lines which clearly cannot approximate the physical integrity of the boundary into the implementation of lattice Boltzmann simulation. This incomplete approximation, especially in high Re number flows can rise to vortices that are unrealistic in the current boundary followed by an analysis of the total area affected by the error. Therefore, in this section a new method introduced by Mohammadipoor *et al.* [15] is employed here which is described below.

In such circumstances, the analysis of the curved line requires a new design. It is should be a design which despite the broken lines as the geometry of the flow, can simulate the physical boundary effect on the curve flow analysis. The introduction of such a scheme is the subject of this section of the paper.

In general terms, when a boundary curve is matched with lattice Boltzmann, nodes will be divided into two areas: nodes that are outside the boundaries of the curve and are the place for fluid and the other are the nodes that are outside the scope of the flow and a place for solid. In Fig. 2, the first group is shown as filled solid circles and the second group is shown as hollow circles. From now on, the subtitles w will be used to show parameters of the boundary curves.

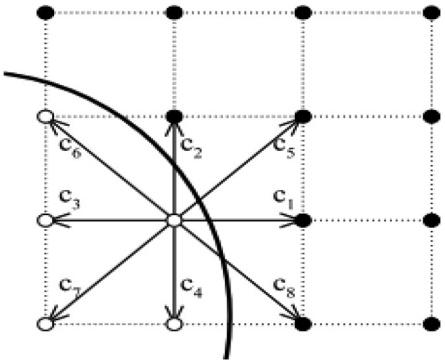

Fig. 2 *Position of curved boundary due to nodal points [15]*

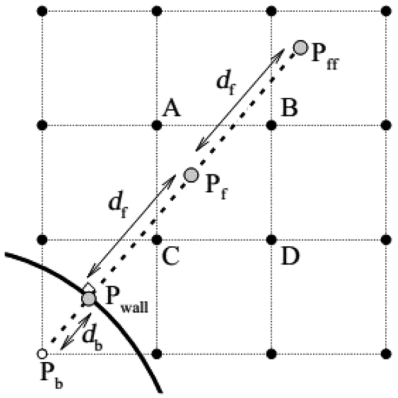

Fig. 3 *Reference nodes on the normal vector to boundary [15]*

It is clear that from among all the nodes on the solid part, only the adjacent nodes in the curve boundary are effective in flow analysis. These nodes in this paper are called as the boundary nodes and their related parameters will be specified with subtitles b.

Border distribution functions in the nodes must be determined in such a way that the result is the simulation of the desired condition on the boundary curve. For this purpose, it is necessary to extrapolate the macroscopic properties of the boundary nodes (M_b) due to the required amount of the property on the curve boundary (M_w) and the value of the property in the nearest node to the wall (M_f). This extrapolation requires two reference points; one is located in solution and another one on the curves boundary. Determining the boundary curve is the most important step in the simulation.

Since all efforts to simulate the curve even during extrapolation has been the relatedness of the nodal points of the lattice, setting the reference is limited to the point c_i of the microscopic lattice speed in a way that the border crossing points of the curve with microscopic lattice speed are considered criteria for selection of reference points for the boundary nodes p_b. In such circumstances, the speed vector with the minimum distance to the intersection of the boundary nodes or velocity vector with the lowest point of the normal vector border are selected as the extrapolation direction. Since the distribution of microscopic velocity covers the range of 360° with only eight velocity vector, the lack of matching to extrapolate to normal direction is likely to be common.

In such circumstances of extrapolation values especially when the boundary condition is of the second type (Newman), the extrapolation is associated with the error. The new design which has been introduced in this paper, by leaving aside the lattice node in the selection of reference points, the constant adaptation to enable normal extrapolation becomes possible. This means that at any point, the boundary line can be expected as perpendicular to the boundary (the boundary normal vector). Intersection of this line with the curve boundary indicates the first reference point (p_w). The second reference point (p_r) is elected on a vertical line and a distance from the first d_f. These are shown in Fig. 3. The assessed property values, in the first reference point (M_w) located on the border of the details (boundary condition) is the known part of the problem. To determine the value of property in the second reference point (M_f), the linear interpolation on four points of A, B, C and D including points of reference is used.

$$M_f = M_C(X_B - X_f)(y_B - y_f)/\delta x^2 + M_D(X_f - X_A)(y_A - y_f)/\delta x^2 + M_A(X_D - X_f)(y_f - y_D)/\delta x^2 + M_B(X_f - X_C)(y_f - y_C)/\delta x^2 \quad (13)$$

Revealing the M_f and M_w values at reference points, the macroscopic properties of the border are calculated by linear extrapolation

$$M_b = \left[1 + \frac{d_b}{d_r}\right]M_w - \frac{d_b}{d_f}M_f \quad (14)$$

In this regard, d_b as shown in Fig. 3 is the distance from the node boundary to the curve boundary that it called the border since then and d_f is the distance between two points of reference in the field of fluid. The distance should be chosen in such a way that four environmental points A, B, C and D exist for the second reference point. Since lattice Boltzmann is square, d_b is always much smaller than $\sqrt{2}\delta x$ so by selecting the greater d_f more than the maximum d_b and to establish $d_f = 2\delta x$, this condition is always provided. If necessary, by selecting the third reference point P_{ff} in $4\delta x$ distance with the first reference, extrapolation can be applied from a quadratic relationship below:

$$M = \left[1 + \frac{d_b}{d_f}\right]\left[1 + \frac{d_b}{2d_f}\right]M_W - \frac{d_b}{d_f}\left[2 + \frac{d_b}{d_f}\right]M_f + \frac{d_b}{2d_f}\left[1 + \frac{d_b}{d_f}\right]M_{ff} \quad (15)$$

In most works done in the field of curve boundary simulation, extrapolation requires the use of two separate equations proportional to the distance from the edge of the boundary nodes to boundary curve which in case of changing extrapolation can be followed by drastic changes in the distribution functions [16, 17] and even in some cases a measure of exchange of extrapolation relationship can affect the accuracy of the results [18]. However, in the model presented in this paper, only one equation (14) or (15) is sufficient to extrapolate the macroscopic properties of the boundary node. From the value calculated by applying M_b on the boundary nodes, one can simulate curve boundary effects.

In other words, the simulation of the curve boundary is simply a matter of applying the calculated values from (14) or (15) on the boundary nodes. The plan is quite general and will be applicable for each of the lattice Boltzmann models. In case of using lattice Boltzmann model to simulate fluid flow, macroscopic properties of M can be velocity, pressure and temperature of the fluid.

4 No-slip boundary condition

According to the design presented in the previous section, the boundary curve simulation requires implementing the macroscopic values calculated from (13) or (14) in boundary nodes. In LBM unlike conventional CFD methods with the appointment of macroscopic boundary conditions is not done using the boundary nodes. Instead, a specified series of distribution functions are selected on

doi: 10.1049/joe.2017.0894

boundary node the effect of which is equivalent to the desired amount of macroscopic boundary.

The specific fluid flow is discussed in this section and macroscopic properties that should be allocated to boundary nodes are the fluid velocity. The purpose of this section is to introduce new models of boundary condition in which the fluid velocity at the boundary nodes is without any undesired slip of the required U_b velocity (rate obtained from extrapolation).

In the boundary node after streaming the distribution functions area outside the settlement into boundary nodes which are unknown, the task of the model is to determine the unknown functions proportional to the desired velocity of the boundary node. For example, in Fig. 4, the unknown functions for a boundary node are located on a flat wall shown in dots. Analysis of Chapman–Enskog which is the link between lattice Boltzmann equation with the Navier–Stokes equation is based on the development of power distribution function

$$f = \sum_{n=0} \varepsilon^n f^n = f^0 + \varepsilon f^{(1)} + o\left(\varepsilon^2\right) \tag{16}$$

In extension, ε is the Knudsen number and f^0 is the equilibrium distribution function.

5 Results and discussion

5.1 Flow around a circular cylinder

We here consider solving the problem of uniform flow past a circular cylinder by means of the LBM. In a special limited range of the Re number, a pair of vortices appears behind the cylinder. The formation of these vortices is very sensitive to the type of boundary model used for the interaction between the cylinder and the neighbouring virtual fluid particles. The important task in the formulisation of the present problem is the treatment of the boundary condition between the cylinder and the virtual fluid particles in the neighbouring lattice sites in addition to the outer boundary conditions. The two-dimensional circular cylinder with diameter D is fixed at the origin of the coordinate system.

In this section, two-dimensional flow passing over a cylinder at Re numbers 20 and 40 are evaluated. Re number in this flows is defined based on the free-stream velocity (U_0) and the cylinder diameter (D) as $\mathrm{Re} = U_0 D/\nu$.

The cylinder periphery includes 40 boundary nodes. Flow rate at the entrance equals to the fixed value of $u = U_0$ and the rapid changes in the flow path are ignored ($\partial U/\partial x = 0$).

It is known that the flow field for outer flow problems is significantly distorted unless a sufficiently large simulation region is used. According to Fig. 5, in the case of Re = 20, the length of the pair of vortices is approximately the same as the cylinder diameter, and the formation of these vortices is quite sensitive to the outer boundary condition that has been adopted.

The input voltage is set to zero. In order to apply the second type of boundary condition, the velocity gradient has changed to the first boundary condition. Finally, its implementation as an inlet boundary condition is done by the help of no-slip boundary condition model presented in this paper. After the first step, a cylindrical border was recognised by the program and no-slip boundary condition is satisfied. Upper and lower boundaries have the periodic boundary condition and to establish a condition of no slip on the cylinder, the boundary condition of the present model is used. Magnified flow lines and vortices formed behind the cylinder for Re numbers 20 and 40 are shown in Fig. 5. Due to the low Re number of the area behind the cylinder, it has a steady and symmetrical state.

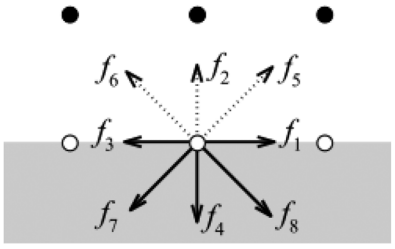

Fig. 4 *Distribution functions in a boundary node*

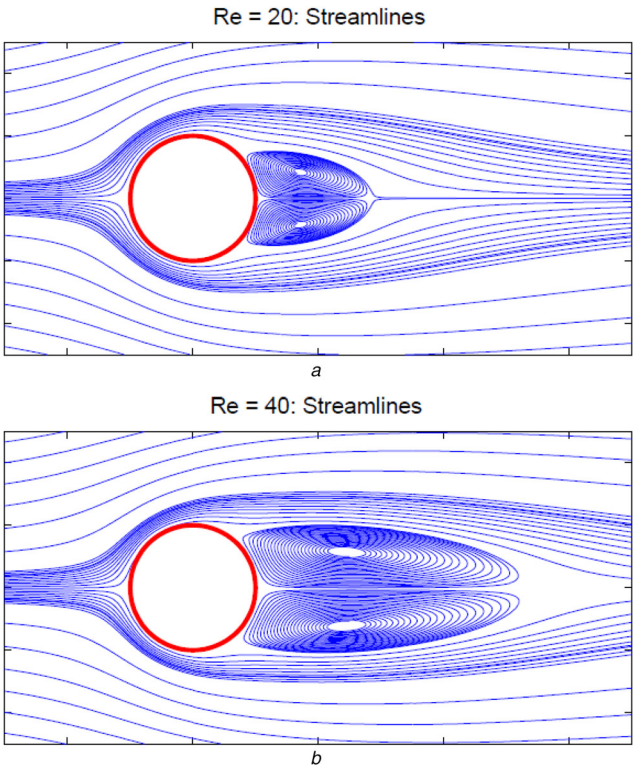

Fig. 5 *Magnified flow lines and vortices formed behind the cylinder for Re numbers 20 and 40*

Table 1 Drag coefficient for Re numbers 100 and 200

C_D	Re = 100	Re = 200
Calhoun [19]	1.33 ± 0.014	1.17 ± 0.058
present study	1.37 ± 0.009	1.34 ± 0.030

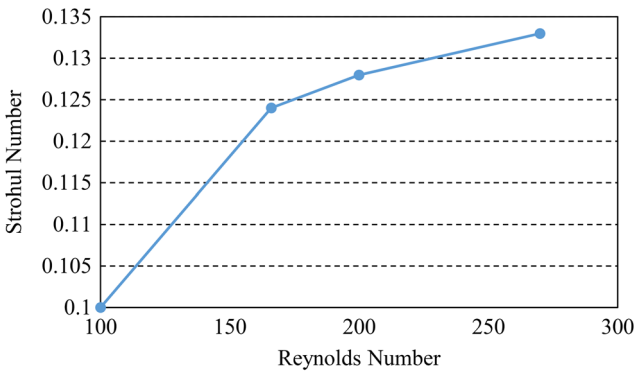

Fig. 6 *Strohul number for different Re number*

doi: 10.1049/joe.2017.0894

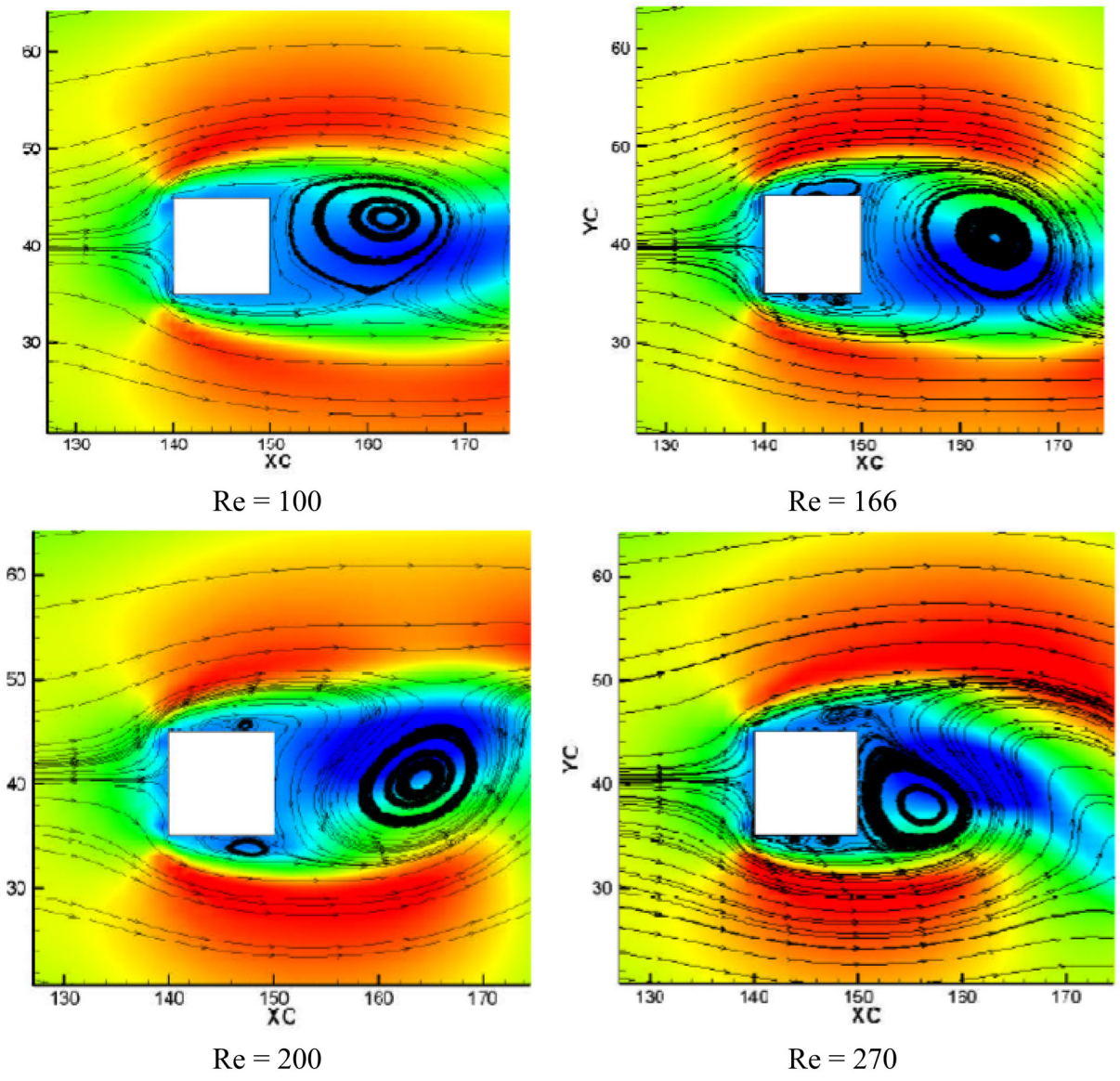

Fig. 7 *Streamlines around the square cylinder in different Re numbers*

Table 1 shows the drag coefficient for Re numbers 100 and 200 with other numerical results are compared. Re = 100 for the average drag coefficient obtained by simulation study, somewhat larger than the value obtained by the authorities (Calhoun [19]). This difference, however, is low at about 1–3%.

5.2 Flow around a square cylinder

In this part, flow around a square cylinder with the dimension of $d \times d$ is investigated in the Re number between 100 and 300. The Re number is defined similarly to circular cylinder, i.e. $\mathrm{Re} = U_0 d/\nu$. Based on empirical observations and numerical simulations, the domain of solving the vortex shedding process occurs with the two-dimensional transient flow. It should be noted that in Re above 300, the flow has three-dimensional structures, and the two-dimensional solution leads to non-physical results. A 10×10 lattice unit is applied to the square cylinder together with no-slip boundary condition.

The Strouhal (St) number is defined according to the following equation:

$$\mathrm{St} = \frac{fd}{U_0} \tag{17}$$

where f is the wake frequency. This frequency is determined by using unsteady spectral analysis of x-component of flow velocity at different points and behind the cylinder. The St numbers for different Re numbers have been shown in Fig. 6.

Fig. 7 displays the streamlines around the square cylinder in different Re numbers. It is noteworthy that the flow structure around the cylinder changes by changing the Re number. For Re = 166, the small secondary vortices are created on the top and button parts of cylinder.

6 Conclusion

In this paper, a new boundary condition for simulation of the curved boundaries in LBM is provided. The new boundary condition model is based on extrapolation of macroscopic properties with the help of only one equation to prevent the drastic changes of distribution functions due to the numerous extrapolation equations. Since the macroscopic properties of the boundary condition model are based on extrapolation, its application is not limited to the flow and would be applicable to all physical problems. In this study, LBM was used to simulate the flow around a rigid cylinder in two-dimensional and unsteady form. Now compare the numerical results with experimental and numerical results of the past studies

doi: 10.1049/joe.2017.0894

obtained using previous methods which reflects the ability of this method to simulate different types of flows. The analysis of the results has been done for different Re numbers. Summary of the most important results of this paper are as follows.

The results of the present numerical simulations showed the resultant symmetric vortex of the cylinder in viscosity of the flow for the Re number smaller than the critical amount.

In this study, we have identified a set of instability in the Reynolds number of about 50. According to previous studies, the cylinder starts to be instable in critical Re about $\mathrm{Re} = 46 \pm 1$. For Re numbers greater than this amount, the instability of the cylinder increases and grows over time, leading to the phenomenon of Karman vortex separation.

For the Re numbers of 20 and 40 for the flow lines, it was shown that due to the low Re number in this area, the wake area behind the cylinder has a steady state and is symmetrical.

7 References

[1] Succi S.: 'The lattice Boltzmann equation for fluid dynamics and beyond' (Clarendon Press, Oxford, 2001)

[2] Rothman D.H., Zaleski S.: 'Lattice-gas cellular automata, simple models of complex hydrodynamics' (Cambridge University Press, Cambridge, 1997)

[3] Rivet J.P., Boon J.P.: 'Lattice gas hydrodynamics' (Cambridge University Press, Cambridge, 2001)

[4] Chopard B., Droz M.: 'Cellular automata modeling of physical systems' (Cambridge University Press, Cambridge, 1998)

[5] McNamara G., Zanetti G.: 'Use of the Boltzmann equation to simulate lattice gas automata', *Phys. Rev. Lett.*, 1998, **61**, (5), pp. 23–32

[6] Chen S., Doolen G.D.: 'Lattice Boltzmann method for fluid flows. *Annu. Rev. Fluid Mech.*, 1998, **30**, (1), pp. 329–364

[7] Succi S.: 'The lattice Boltzmann equation for fluid dynamics and beyond' (Oxford University Press, Oxford, 2001)

[8] Sukop M.C., Thorne D.T.: 'Lattice Boltzmann modeling: an introduction for geoscientists and engineers' (Springer, Heidelberg, 2007)

[9] Zhang J.F., Johnson P.C., Popel A.S.: 'Red blood cell aggregation and dissociation in shear flows simulated by lattice Boltzmann method', *J. Biomech.*, 2008, **41**, pp. 47–55

[10] Cheng Y., Zhang H.: 'Immersed boundary method and lattice Boltzmann method coupled FSI simulation of mitral leaflet flow', *Comput. Fluids*, 2010, **39**, (5), pp. 871–881

[11] Hyakutake T., Ohkawa S., Mohri S., *ET AL.*: 'Lattice Boltzmann analysis of microvascular constriction flow including red blood cell and liposome-encapsulated hemoglobin', *Theor. Appl. Mech. Japan*, 2008, **56**, pp. 215–224

[12] Dupuis A., Chatelain P., Koumoutsakos P.: 'An immersed boundary-lattice-Boltzmann method for the simulation of the flow past an impulsively started cylinder', *J. Comput. Phys.*, 2008, **227**, (9), pp. 4486–4498

[13] Zhang J.F., Johnson P.C., Popel A.S.: 'An immersed boundary lattice Boltzmann approach to simulate deformable liquid capsules and its application to microscopic blood flows', *Phys. Biol.*, 2007, **4**, (4), pp. 285–295

[14] Wu J., Shu C.: 'An improved immersed boundary-lattice Boltzmann method for simulating three-dimensional incompressible flows', *J. Comput. Phys.*, 2010, **229**, pp. 5022–5042

[15] Mohammadipoor O.R., Niazmand H., Mirbozorgi S.A.: 'Alternative curved-boundary treatment for the lattice Boltzmann method and its application in simulation of flow and potential fields', *Phys. Rev. E*, 2014, **89**, p. 013309

[16] Zhu L., He G., Wang S., *ET AL.*: 'An immersed boundary method based on the lattice Boltzmann approach in three dimensions with application', *Comput. Math. Appl.*, 2011, **61**, (12), pp. 3506–3518

[17] Yu D., Mei R., Luo L.S., *ET AL.*: 'Viscous flow computations with the method of lattice Boltzmann equation', *Prog. Aerosp. Sci.*, 2003, **39**, (5), pp. 329–367

[18] Kao P.H., Yang R.J.: 'An investigation into curved and moving boundary treatments in the lattice Boltzmann method', *J. Comput. Phys.*, 2008, **227**, (11), pp. 5671–5690

[19] Calhoun D.: 'A Cartesian grid method for solving the two-dimensional stream function-vorticity equations in irregular regions', *J. Comput. Phys.*, 2002, **176**, pp. 231–275